Front. Energy Power Eng. China 2010, 4(4): 546–552
DOI 10.1007/s11708-010-0116-8

RESEARCH ARTICLE

Yufei MAO, Liejin GUO, Bofeng BAI, Ximin ZHANG

Convective heat transfer in helical coils for constant-property and variable-property flows with high Reynolds numbers

Abstract Forced convection heat transfer of single-phase water in helical coils was experimentally studied. The testing section was constructed from a stainless steel round tube with an inner diameter of 10 mm, coil diameter of 300 mm, and pitch of 50 mm. The experiments were conducted over a wide Reynolds number range of 40000 to 500000. Both constant-property flows at normal pressure and variable-property flows at supercritical pressure were investigated. The contribution of secondary flow in the helical coil to heat transfer was gradually suppressed with increasing Reynolds number. Hence, heat transfer coefficients of the helical tube were close to those of the straight tube under the same flow conditions when the Reynolds number is large enough. Based on the experimental data, heat transfer correlations for both incompressible flows and supercritical fluid flows through helical coils were proposed.

Keywords convective heat transfer, helical coils, high Reynolds number, supercritical pressure, variable property

1 Introduction

With the advantages of high efficiency in heat transfer and compactness in structure, helical coils are extensively used in engineering applications such as heat exchangers, steam generators, and chemical reactors. For these reasons, heat transfer of fluids flowing in helical pipes has become a research subject of significant engineering interest during the past decades.

As fluid flows through a curved pipe, secondary flows occur in planes normal to the main flow by the action of centrifugal force, resulting in a high increase in friction factors and heat transfer coefficients compared with that in an equivalent straight pipe. Many studies were conducted on the convective heat transfer characteristics in helical coils. A number of heat transfer correlations for the fully developed incompressible turbulent flow of single-phase fluids were published, such as those of Merkel [1], Seban and Mclanghlin [2], Rogers and Mayhew [3], Mori and Nakayama [4], and Guo et al. [5]. However, most correlations available for helical coils were obtained in the low Reynolds number region ($Re < 100000$). Further work is required to fully understand heat transfer in the higher Reynolds number region.

The flow of fluid at normal pressure is collected as a constant-property (incompressible) flow. In empirical correlation, the relationship between Nusselt, Reynolds, and Prandtl numbers remains more or less the same along the course of the flow. The peculiarity of heat transfer of supercritical fluids is primarily attributed to the significant variation of fluid thermophysical properties in the pseudo critical region. For supercritical fluid flows characterized by significant property variations, the conventional heat transfer correlations are inapplicable. According to the recent survey of Pioro and Duffey [6], a majority of previous experimental studies deal with the heat transfer of supercritical pressure fluids in straight pipes, while research devoted to heat transfer in helical pipes is sparse. With the development of supercritical fluid technology, a systematic study of the convective heat transfer to supercritical fluid flows in helical coils is needed.

We aim to achieve a general understanding of the single-phase forced convection heat transfer to turbulent flow of water in helical coils within a wide range of the Reynolds number. Experiments are conducted on both constant-property flows at normal pressures and variable-property flows at supercritical pressures.

2 Experimental facility and procedure

Figure 1 shows a schematic diagram of the high-pressure

Received April 30, 2010; accepted June 5, 2010

Yufei MAO (✉), Liejin GUO, Bofeng BAI, Ximin ZHANG
State Key Laboratory of Multiphase Flow in Power Engineering, Xi'an Jiaotong University, Xi'an 710049, China
E-mail: yfmao@stu.xjtu.edu.cn

water test loop. The test loop is primarily composed of a water tank to provide deionized water for the experiments, a high-pressure plunger pump to supply power for the fluid flow, a series of orifice flowmeters to measure water mass flow rate, a regenerative heat exchanger and three preheaters to collectively raise the water temperature before water enters the test section, a heat transfer test section, and a water-cooled condenser to cool the high-temperature working fluid before it returns to the water tank. Both the preheaters and the test section are electrically heated by running AC current through the tube walls. The electrical power delivered to the preheaters and the test section is 460 $(180 + 180 + 100)$ kW and 100 kW, respectively. The whole test loop is thermally insulated from the atmosphere to minimize heat loss.

The schematic diagram of the test section is illustrated in Fig. 2. The section is vertically oriented with the water flowing against gravity. The section is made of a 10-m long seamless stainless steel tube with an inner diameter of 10 mm, outer diameter of 14 mm, coil diameter of 300 mm, and pitch of 50 mm. The heated test section is 7.2 m long, and is followed and preceded by two short unheated sections to eliminate the effect of the entry and exit conditions. Three armored K-type thermocouples with a diameter of 3 mm are installed in the core of the tube to measure the bulk temperature of the fluid at the inlet, middle, and outlet of the heated section. A total of 76 K-type thermocouples with a diameter of 0.5 mm are welded on the outside surface of the heated section at the 15 thermocouple stations to measure wall temperature. Four thermocouples are located at the No. 1–No. 11 stations and eight thermocouples are located at the No. 12–No. 15 stations. The first and seventh stations are located 600 mm from the inlet and middle of the heated section, respectively. The distance between the adjacent No. 1–No. 6 and No. 7–No. 12 stations is 500 mm. The last (15th) station is located 100 mm from the outlet of the heated section. The distance between the adjacent stations of No. 13–No. 15 is 100 mm. Uncertainty in the bulk and wall temperatures measured by the thermocouples is about $\pm 0.5\%$.

Absolute pressures in the inlet and outlet of the heated test section are measured by two ST3000 Series pressure transducers within the range of 0–40 MPa. Estimated accuracy of the pressure measurements is about $\pm 0.5\%$. Mass flow of the working fluid through the test section is measured by the three orifice flowmeters within different ranges attached to three ST3000 Series differential pressure transducers within the range of 0–99.6 kPa. These orifice flowmeters are calibrated by the weighting method. The uncertainty is estimated to be less than 3%. Total electrical power supplied to the test section and the preheaters is calculated from the measured voltage and current through each heated section. The estimated uncertainty is $\pm 3.25\%$. Maximum uncertainty in heat transfer measurements is $\pm 5.08\%$. The signals of the system pressure, mass flow, and temperature of the tube wall and the bulk fluid, and the input heating powers of the test section and the preheaters are monitored and recorded via an isolated measurement pod (IMP) data acquisition system.

Bulk fluid temperature at each thermocouple station is determined according to the bulk fluid enthalpy at the local station. Bulk enthalpy is calculated from the given inlet, middle, or outlet bulk enthalpy, as well as from the electrical heat input to the station and the mass velocity. Heat efficiency of the test section, determined as the ratio of the absorption of heat of water divided by the input electric power, is within 0.9 to 0.95. The inside wall temperature is estimated from the measured outside wall temperature by the space marching method in relation to the inverse heat conduction problems [7]. Thermophysical

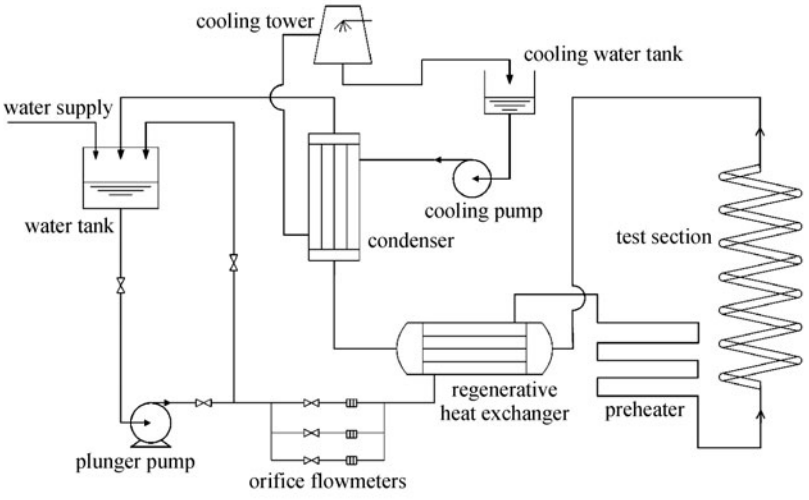

Fig. 1 Schematic diagram of test loop

properties of the water are obtained from the source code of the IAPWS-95 formulation [8]. Boundary condition of the uniform heat flux is assumed for the heated test section. Circumferential average heat transfer coefficient at the position z along the tube is defined as

$$h_z = q_w/(\overline{T}_{w,z} - T_{b,z}), \quad (1)$$

where $\overline{T}_{w,z}$ is the cross-sectional average inner wall temperature of the tube at position z.

3 Results and discussion

3.1 Convective heat transfer for constant-property flows

Experiments on single-phase constant-property flows are performed over a range of system pressures from 8 to 15 MPa, mass velocities from 1200 to 5000 kg/(m^2·s), and wall heat fluxes from 100 to 400 kW/m^2. These cover the Reynolds number ranging from 3.5×10^4 to 5×10^5. The experimental data are compared with the predictions by three conventional correlations for helical coils and the well-known Dittus-Boelter correlation for straight pipes. These correlations are listed as follows:

the Merkel correlation

$$Nu_b = 0.023 \cdot Re_b^{0.8} \cdot Pr_b^{0.4} \cdot [1 + 3.54(d/D)], \quad (2)$$

the Rogers-Mayhew correlation

$$Nu_b = 0.023 \cdot Re_b^{0.85} Pr_b^{0.4} (d/D)^{0.1}, \quad (3)$$

the Mori-Nakayama correlation

$$Nu_b = \frac{1}{41} Re_b^{5/6} Pr_b^{0.4} \left(\frac{d}{D}\right)^{1/12} \cdot \left\{1 + \frac{0.061}{[Re_b (d/D)^{2.5}]^{1/6}}\right\}, \quad (4)$$

and the Dittus-Boelter correlation

$$Nu_b = 0.023 \cdot Re_b^{0.8} Pr_b^{0.4}. \quad (5)$$

The experimental data are compared with the predictions by different correlations and presented in Fig. 3. Results show that the experimental data are in good agreement with the predictions by the Rogers-Mayhew correlation and the Mori-Nakayama correlation when the Reynolds number is approximately less than 1.2×10^5. The data are in good agreement with the prediction by the Merkel correlation when the Reynolds number is within the range of 1.2×10^5 to 2×10^5. Heat transfer coefficients can be directly predicted by the Dittus-Boelter correlation when the Reynolds number is above 2×10^5. Therefore, the effect of secondary flow in helical coils on the convective heat transfer diminishes as the Reynolds number increases and can be neglected when the Reynolds number is large enough. This is validated by the study of Guo et al. [5].

Based on the results, an empirical method for the calculation of heat transfer coefficients within different ranges of the Reynolds number to constant-property flows in helical coils is proposed as Eq. (6). Figure 4 demonstrates the comparison of the prediction by Eq. (6) with the experimental data. All deviations between the prediction and the experimental data are almost within ±15%. Average relative deviation is about 5.26%.

$$Nu_b = \begin{cases} 0.023 Re_b^{0.85} Pr_b^{0.4} (d/D)^{0.1}, \\ \quad 3.5\times10^4 \leqslant Re \leqslant 1.2\times10^5, \\ 0.023 Re_b^{0.8} Pr_b^{0.4} \left(1 + 3.54\dfrac{d}{D}\right), \\ \quad 1.2\times10^5 \leqslant Re \leqslant 2\times10^5, \\ 0.023 Re_b^{0.8} Pr_b^{0.4}, \\ \quad 2\times10^5 \leqslant Re \leqslant 5\times10^5. \end{cases} \quad (6)$$

3.2 Convective heat transfer for variable-property flows

Experiments on the variable-property flows are conducted with the system pressure ranging from 23.5 to 26.5 MPa, mass velocity from 800 to 1600 kg/(m^2·s), wall heat flux from 100 to 400 kW/m^2, and bulk enthalpy from 800–2900 kJ/kg, covering the bulk Reynolds number from 5.5×10^4 to 5.5×10^5. The effects of control variables (e.g., system pressure, mass velocity, and wall heat flux) on the convective heat transfer of supercritical pressure water in helical coils are systematically investigated.

The experimental heat transfer coefficients plotted against the bulk enthalpy are shown in Figs. 5–7. Heat transfer coefficient is remarkably increased in the pseudo critical region and has a maximum value in the vicinity of the pseudo critical point where the isobaric specific heat attains a maximum value. Figure 5 reveals the effect of system pressure on heat transfer. The heat transfer coefficient in the pseudo critical region (especially near the pseudo critical point) increases as the pressure achieves values closer to the critical pressure. The variation of the heat transfer coefficient with the pressure and bulk temperature resembles the way the isobaric specific heat varies with pressure and temperature. According to Fig. 6, the effect of mass velocity on heat transfer for variable-property flows at supercritical pressures is similar to that of the constant-property flows at normal pressures. The higher the mass velocity, the stronger the convection, and, hence, the higher the heat transfer coefficient. Figure 7 shows the effect of wall heat flux on heat transfer. With increasing heat flux, the temperature difference between the wall and the bulk increases. However, for supercritical fluid flows, the growth of the temperature difference is greater than the increase of the heat flux. Therefore, the heat transfer coefficient decreases as the heat flux is increased.

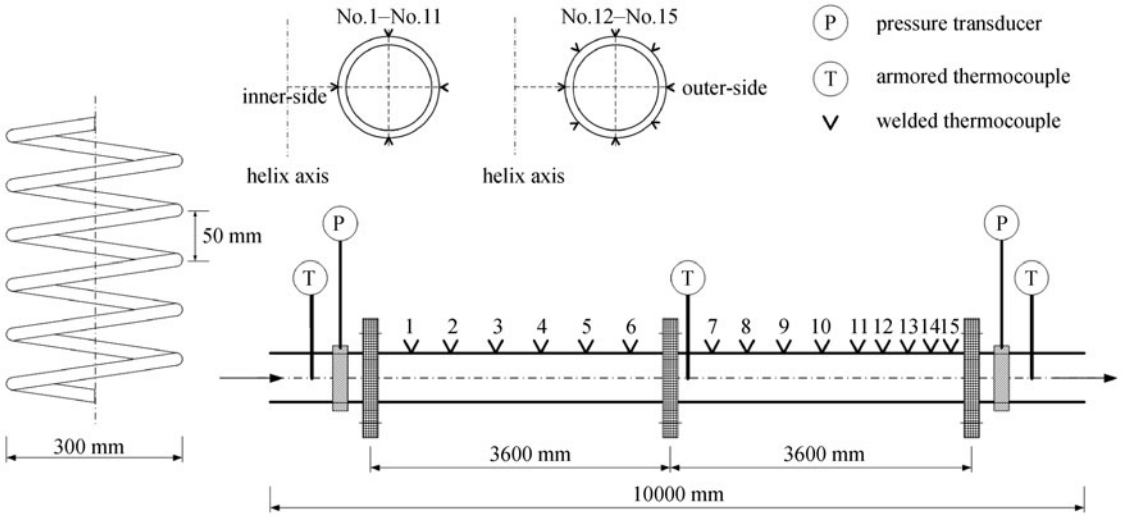

Fig. 2 Schematic diagram of test section

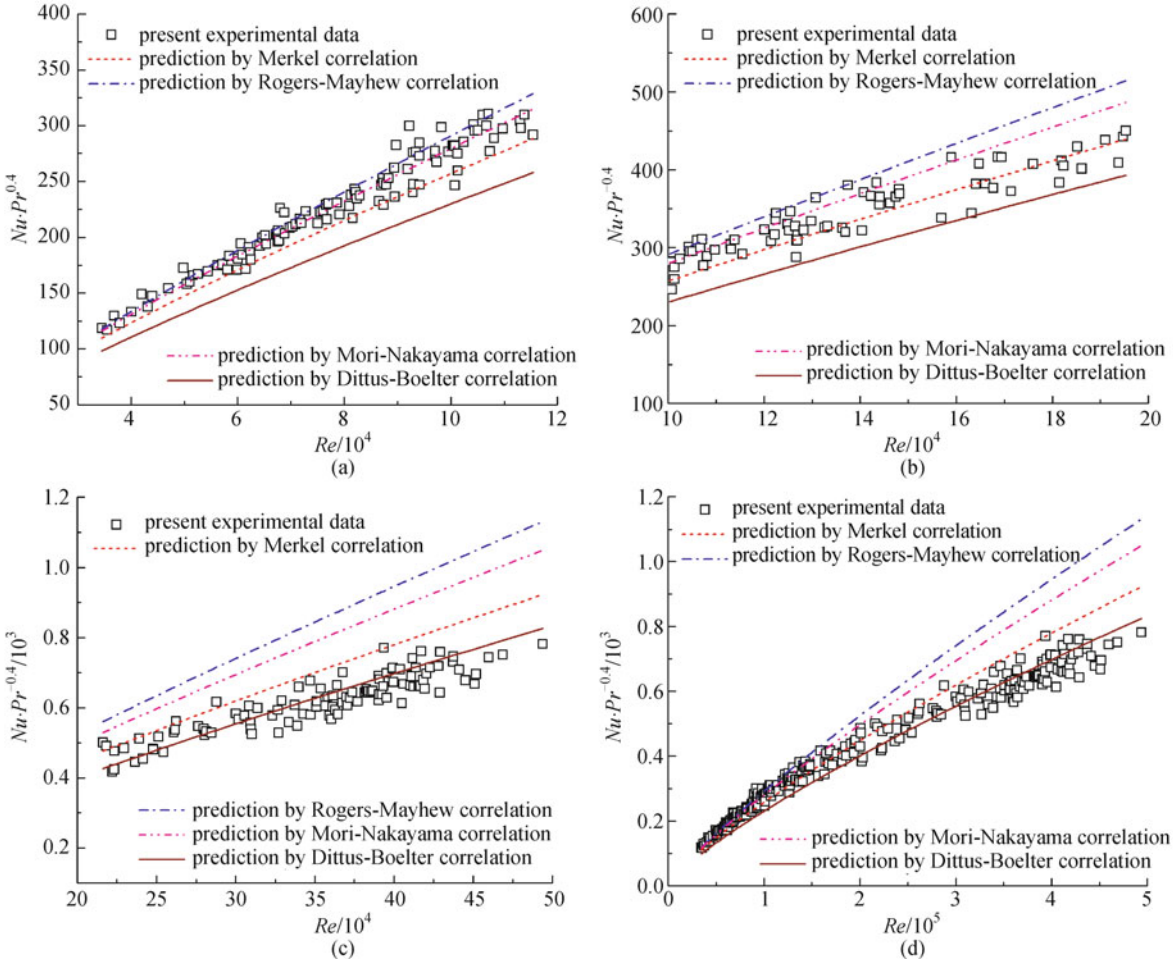

Fig. 3 Experimental results for constant-property flows
(a) $Re = 1.2\times10^5$–3.5×10^5; (b) $Re = 10^5$–2×10^5; (c) $Re = 2\times10^5$–5×10^5; (d) $Re = 3.5\times10^4$–5×10^5

The present data derived from the helical tube (p = 24 MPa, G = 1200 kg/(m^2·s), q_w = 400 kW/m^2, d = 10 mm) experiment are compared with the previous experimental data of the straight tube experiment by Yamagata [9] (p = 24.5 MPa, G = 1200 kg/(m^2·s), q_w = 465 kW/m^2, d = 10 mm) and by Xu [10] (p = 23 and 25 MPa, G =

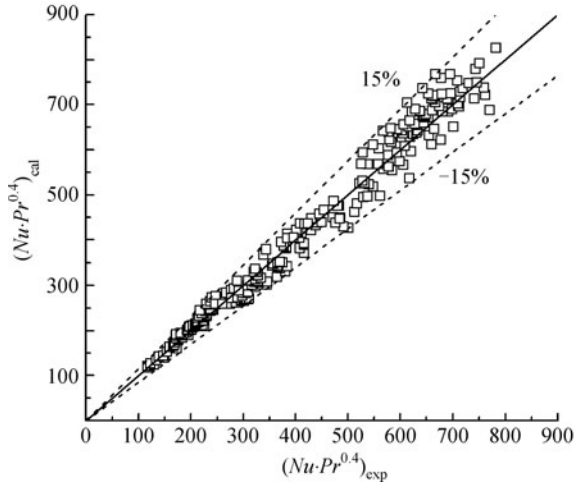

Fig. 4 Comparison of prediction by Eq. (6) with experimental data

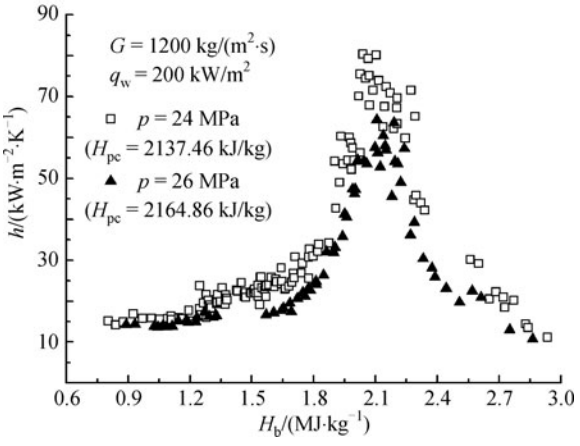

Fig. 5 Effect of system pressure on heat transfer for supercritical fluid flows

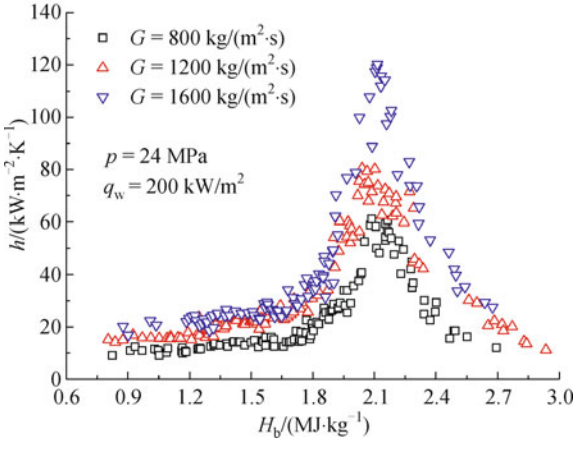

Fig. 6 Effect of mass velocity on heat transfer for supercritical fluid flows

1200 kg/(m^2·s), $q_w = 400$ kW/m^2, $d = 12$ mm). The comparison results are shown in Fig. 8. For the supercritical

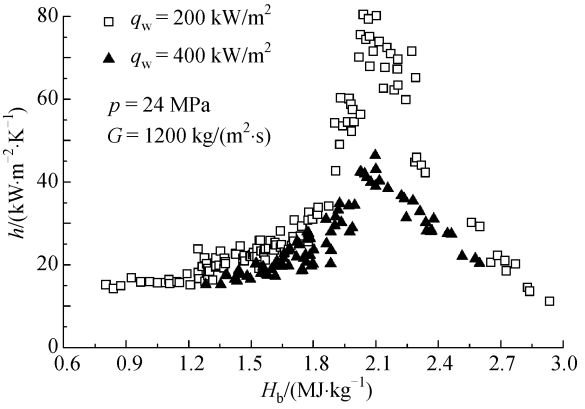

Fig. 7 Effect of wall heat flux on heat transfer for supercritical fluid flows

fluid flows with low or moderate heat fluxes and with relatively high mass velocities in the pseudo critical region, the heat transfer coefficients of the helical tube are quite close to those of the straight tube on the same flow conditions. This means that the contribution of secondary flow in helical coils to the heat transfer is suppressed compared with that of the property variation and the forced convection.

Based on the 615 experimental data points, a correlation for the calculation of the convective heat transfer coefficients of supercritical pressure water flowing in the helical coils is obtained as follows:

$$Nu_b = 0.0161 Re_b^{0.848} \overline{Pr}_b^{0.632} (\rho_w/\rho_b)^{0.851}, \quad (7)$$

where

$$\overline{Pr}_b = \overline{c}_p \mu_b/\lambda_b,\ \overline{c}_p = (H_w - H_b)/(T_w - T_b). \quad (8)$$

The comparison between the prediction by Eq. (7) and the data is shown in Fig. 9. Most of the predicted results are within a deviation of ±20%. Average relative deviation is about 9.78%.

The Yamagata correlation [9] is developed based on the data from an upward vertical flow in a straight tube with an inner diameter of 10 mm. It is expressed as

$$Nu_b = 0.0135 Re_b^{0.85} Pr_b^{0.8} F_c, \quad (9)$$

where the correction term F_c is calculated by

$$\begin{cases} F_c = 1 & \text{for } E > 1, \\ F_c = 0.67 Pr_{pc}^{-0.05} (\overline{c_p}/c_{pb})^{n_1} & \text{for } 0 \leqslant E \leqslant 1, \\ F_c = (\overline{c_p}/c_{pb})^{n_2} & \text{for } E < 0, \\ E = (T_{pc} - T_b)/(T_w - T_b), & \\ n_1 = -0.77(1 + 1/Pr_{pc}) + 1.49, & \\ n_2 = 1.44(1 + 1/Pr_{pc}) - 0.53. & \end{cases} \quad (10)$$

The Yamagata correlation divides heat transfer regimes

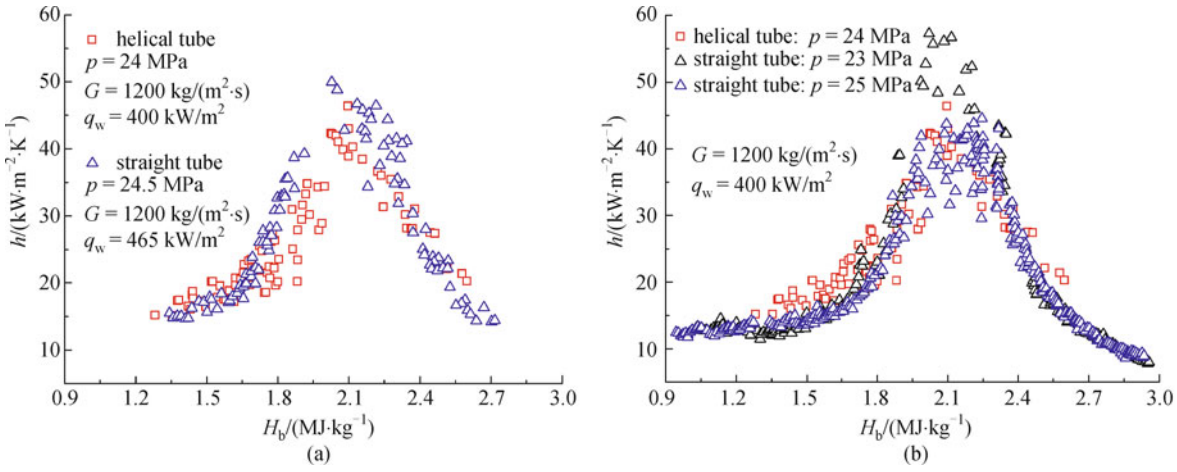

Fig. 8 Comparison of present experimental data of straight tubes with previous experimental data of (a) Yamagata [9] and (b) Xu [10]

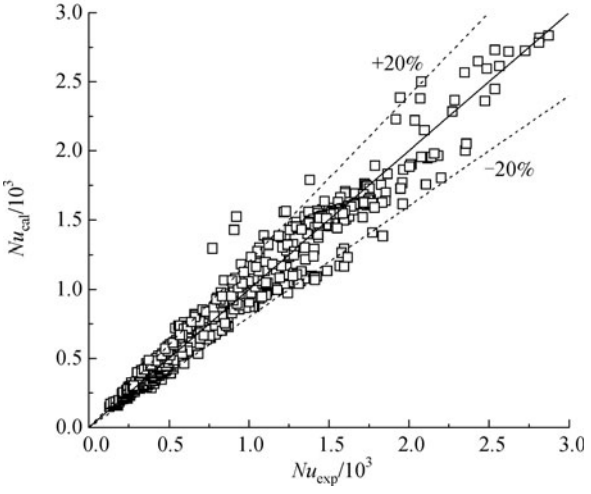

Fig. 9 Comparison of the prediction by Eq. (7) with present experimental data

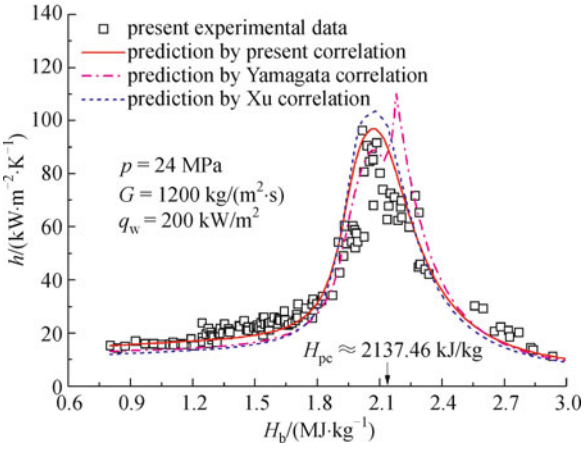

Fig. 10 Comparison of the experimental data with the prediction by different correlations

into various categories for better experimental data fit. However, this method causes discontinuity in the heat transfer coefficients as the wall temperature approaches the pseudo critical temperature.

The Xu correlation [10] is developed based on data from an upward vertical flow in a straight tube with an inner diameter of 12 mm. It is expressed as

$$Nu_b = 0.0068 Re_b^{0.904} \overline{Pr}_b^{0.778} (\rho_w/\rho_b)^{0.884}. \quad (11)$$

Figure 10 shows a comparison of the experimental data [$p = 24$ MPa, $G = 1200$ kg/(m^2·s), $q_w = 200$ kW/m^2, $d = 10$ mm] with the prediction by the present correlation, Yamagata correlation, and Xu correlation. The predicted results of the Yamagata correlation and Xu correlation for straight tubes are seemingly lower than the present experimental data for helical coils when the bulk enthalpy is approximately below 1800 kJ/kg (where the bulk Reynolds number is about 1.97×10^5). They are in relatively good agreement with the experimental data when the bulk enthalpy is above 1800 kJ/kg.

4 Conclusions

We investigated the characteristics of forced convection heat transfer to turbulent flow of water in a helical coiled tube. The following conclusions are derived.

1) For single-phase constant-property flows at normal pressures, the effect of secondary flow in helical coils on convective heat transfer diminishes with the increase in Reynolds number. Heat transfer coefficients for helical coils can be directly predicted by the Dittus-Boelter correlation when the Reynolds number is large enough (above 2×10^5). An empirical method for the calculation of heat transfer coefficients of constant-property flows in helical coils within different Reynolds number ranges is

proposed.

2) The present experimental results for helical coils are basically consistent with those of previous works for straight tubes. Heat transfer in the pseudo critical region is greatly enhanced due to the significant variations in thermophysical properties. The heat transfer coefficient achieves a maximum in the vicinity of the pseudo critical point, and progressively decreases as the system pressure or wall heat flux is increased. The effect of mass velocity on heat transfer for variable-property flows at supercritical pressures is similar to that of constant-property flows at normal pressures. With increasing mass velocity, the heat transfer coefficient is increased.

3) For supercritical fluid flows with low or moderate heat fluxes and relatively high mass velocities, the contribution of the secondary flow in helical coils to heat transfer is also gradually suppressed with increasing bulk enthalpy (or bulk Reynolds number). Heat transfer coefficients for helical coils can be directly predicted by the correlations for straight tubes when the bulk enthalpy is large enough (above 1800 kJ/kg). A heat transfer correlation for supercritical pressure water flowing in helical coils is obtained without consideration of the effect of the coil curvature.

Acknowledgements This work was supported by the National Natural Science Foundation of China for Creative Research Groups (Grant No. 50821064).

Notation

c_p	isobaric specific heat capacity/($J \cdot kg^{-1} \cdot K^{-1}$)
D	coil diameter of the test section/m
d	inner diameter of the test section/m
G	mass velocity/($kg \cdot m^{-2} \cdot s^{-1}$)
H	specific enthalpy/($J \cdot kg^{-1}$)
h	heat transfer coefficient/($W \cdot m^{-2} \cdot K^{-1}$)
Nu	Nusselt number
p	pressure/Pa
Pr	Prandtl number
q	heat flux/($W \cdot m^{-2}$)
Re	Reynolds number
T	temperature/K

Greek symbols

λ	thermal conductivity/($W \cdot m^{-1} \cdot K^{-1}$)
μ	dynamic viscosity/($N \cdot s \cdot m^{-2}$)
ρ	density/($kg \cdot m^{-3}$)

Subscripts

b	bulk condition
cal	calculation
exp	experiment
pc	pseudo critical point
w	wall condition

References

1. Merkel F. Die Grundlagen der Warmeubertragung. Berlin: Springer Publishing Company, 1927
2. Seban R A, Mclanghlin E F. Heat transfer in tube coils with laminar and turbulent flow. International Journal of Heat and Mass Transfer, 1963, 6(5): 387–395
3. Rogers G F C, Mayhew Y R. Heat transfer and pressure loss in helically coiled tubes with turbulent flow. International Journal of Heat and Mass Transfer, 1964, 7(11): 1207–1216
4. Mori Y, Nakayama W. Study on forced convection heat transfer in curved pipes (2nd report, turbulent region). International Journal of Heat and Mass Transfer, 1967, 10(1): 37–59
5. Guo L J, Chen X J, Feng Z P, Bai B F. Transient convective heat transfer in a helical coiled tube with pulsatile fully developed turbulent flow. International Journal of Heat and Mass Transfer, 1998, 41(19): 2867–2875
6. Pioro I L, Duffey R B. Experimental heat transfer in supercritical water flowing inside channels (survey). Nuclear Engineering and Design, 2005, 235(22): 2407–2430
7. Taler J, Zima W. Solution of inverse heat conduction problems using control volume approach. International Journal of Heat and Mass Transfer, 1999, 42(6): 1123–1140
8. Wagner W, Pruß A. The IAPWS formulation 1995 for the thermodynamic properties of ordinary water substance for general and scientific use. Journal of Physical and Chemical Reference Data, 2002, 31: 387–535
9. Yamagata K, Nishikawa K, Hasegawa S, Fujii T, Yoshida S. Forced convective heat transfer to supercritical water flowing in tubes. International Journal of Heat and Mass Transfer, 1972, 15(12): 2575–2593
10. Xu F. Study of water flow and heat transfer characteristics through pipes under supercritical pressure. Dissertation for the Master's Degree. Xi'an: Xi'an Jiaotong University, 2004, 40–42 (in Chinese)